UC Berkeley
SEMM Reports Series

Title
Computational Aspects of One-Dimensional Shape Memory Alloy Modeling with Phase Diagrams

Permalink
https://escholarship.org/uc/item/6qk6m82j

Authors
Govindjee, Sanjay
Kasper, Eric

Publication Date
1998-02-01

eScholarship.org Powered by the California Digital Library
University of California

REPORT NO.
UCB/SEMM-98/03

STRUCTURAL ENGINEERING
MECHANICS AND MATERIALS

COMPUTATIONAL ASPECTS OF ONE-DIMENSIONAL SHAPE MEMORY ALLOY MODELING WITH PHASE DIAGRAMS

BY

SANJAY GOVINDJEE

AND

ERIC P. KASPAR

FEBRUARY 1998

DEPARTMENT OF CIVIL ENGINEERING
UNIVERSITY OF CALIFORNIA
BERKELEY, CALIFORNIA

Computational Aspects of One-Dimensional Shape Memory Alloy Modeling with Phase Diagrams⋆

SANJAY GOVINDJEE†
&
ERIC P. KASPER‡

Structural Engineering, Mechanics, and Materials
Department of Civil and Environmental Engineering
University of California at Berkeley
Berkeley, CA 94720-1710

§ **Abstract**

A constitutive model for martensitic solid-solid phase transformations is developed. Specifically, we investigate and model the one-dimensional behavior of shape memory alloys, with the purpose of capturing both the shape memory effect and the pseudoelasticity effect which are uniquely exhibited by this class of alloys. The model is of the popular phase space type and an appropriate numerical approximation of the constitution is developed which robustly handles arbitrary one-dimensional thermomechanical loading. Heuristics are provided for treating two types of non-uniqueness issues that have been identified to arise with such models. Representative simulations demonstrate the ability of the formulation to capture the essential macroscopic behavior of shape memory alloys. In particular examples are shown solving truss bar and beam finite element problems.

⋆ Research sponsored in part by the Lawrence Livermore National Laboratory under contract # B34085

† Assistant Professor of Civil Engineering

‡ Presently Assistant Professor of Civil Engineering, California Polytechnic State University, San Luis Obispo

§1. Introduction

General Characteristics of Shape Memory Alloys

Shape memory alloys are materials that display a very particular type of martensitic transformation. These transformations are classified as first order diffusionless displacive transformations, and consist of lattice transformations involving a shearing deformation, which results from a cooperative motion of atoms over a small distance; see e.g. FUNAKUBO [1984] or DUERIG ET.AL. [1990]. The movement is such that there exists a one-to-one correspondence between lattice points in the parent phase (austenite) to the lattice points in the product phase (martensite), known as lattice correspondence. The parent phase typically has a high symmetry group whereas the product phase usually has a low symmetry group; e.g. in NiTi alloys the austenite may be cubic and the martensite monoclinic. During the production of martensite from austenite several different orientations of the martensite are from an energetic point of view equally likely to be produced. The differing orientations are often referred to as martensitic variants. The existence of the variants is one of the micromechanical features of these materials that give them their unique material properties since it is possible to convert one variant to another with little added energetic input – an additional transformation process known as reorientation.

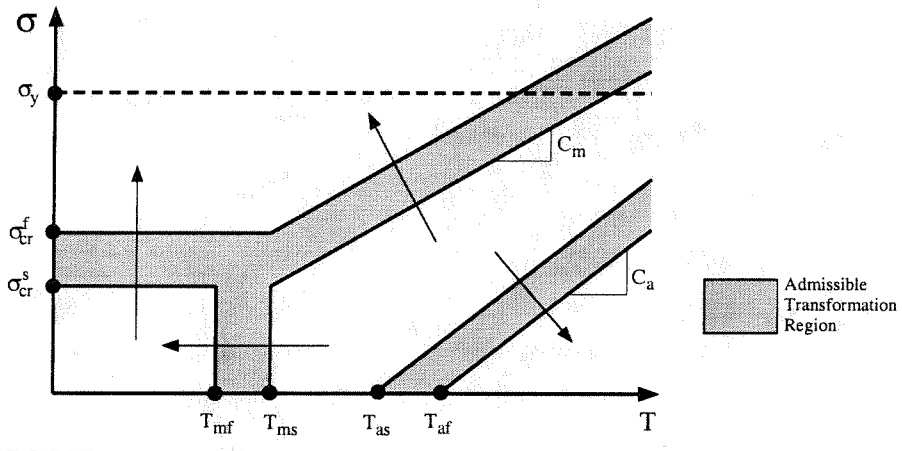

FIGURE 1.1. Phase space diagram depicting transformation zones and their associated values of stress and temperature for activation.

The activation of a martensitic transformation occurs due to the presence of driving forces, either thermal of kinetic. To initiate a transformation, the chemical free energy difference between the parent and product phases must be greater than the necessary free energy barriers, such as transformational strain energy or interface energy. For the determination of when transformations initiate, the space parameterized by stress and temperature is commonly used. The stress-temperature space is referred to as the phase space and is depicted in Figure **1.1** for tensile states of stress. The arrows indicate the direction of travel needed for an active transformation through the shaded transformation

regions, while σ_{cr}^{s} and σ_{cr}^{f} denote the critical start and finish stresses of a martensite reorientation transformation and C_m and C_a represent the slopes of the transformation lines. The transformation temperatures, T_{mf}, T_{ms}, T_{as} and T_{af} indicate the start and finish temperatures at zero stress for martensite and austenite production, respectively. Lastly, σ_y indicates the value of stress above which plastic slip will occur. Dependant upon the path taken within the phase space, certain characteristic features of the stress-strain $(\sigma - \varepsilon)$ response will manifest themselves.

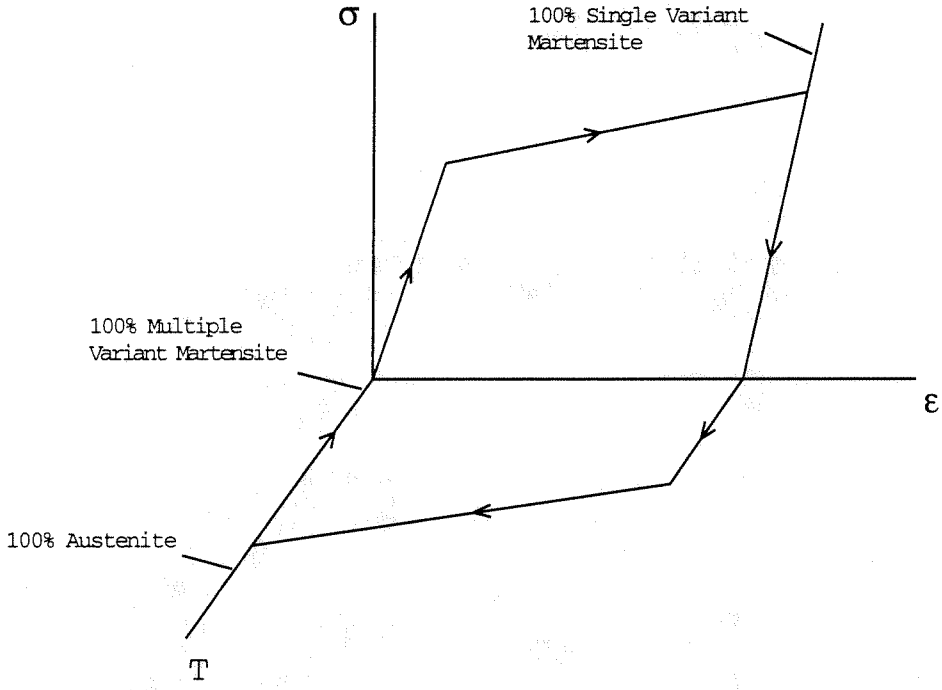

FIGURE 1.2. Shape memory effect. The material begins stress free at a high temperature and is cooled under zero load to form martensite. The specimen is then loaded and unloaded at constant temperature. Lastly, the specimen is heated to return to its original austenitic state.

If austenite is cooled from above T_{af} to below T_{mf} at zero stress the resulting effect will be the creation of a "self accommodating" or "twinned" microstructure. This process begins at T_{ms} and completes at T_{mf}. The ensuing multiple variants which form tend to average the overall deformation to a net zero change in shape on the macroscopic scale (neglecting any thermal expansion). If this material is subsequently mechanically stressed above σ_{cr}^{f} the multiple variants will coalesce into one variant in the preferred direction of loading, in a process known as detwinning or re-orientation. This process begins at σ_{cr}^{s} and finishes at σ_{cr}^{f}. Upon removal of the mechanical load, a permanent deformation is retained in the specimen. If the material is now heated above the critical temperature, T_{af}, it reverts to austenite and completely recovers its original shape — i.e. the so-called shape memory effect. This recovery process begins at T_{as} and completes at T_{af}; see Figure

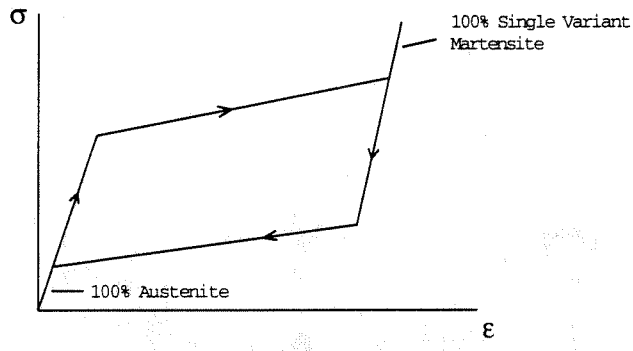

FIGURE 1.3. Pseudoelastic process begins stress free at a high temperature and is then loaded to a martensitic state and unloaded at constant temperature to its original austenitic state.

1.2 for a schematic of the process just described in the temperature-strain-stress space. Note that the amount of recoverable strain can easily exceed 5%.

When the temperature is above the finish temperature T_{af} and the specimen is loaded mechanically above a critical stress level σ_{mf}†, austenite will transform into a single variant martensite oriented in the direction of loading, accompanied by a large macroscopic strain. The strain is recovered upon removal of the mechanical load, since martensite is not stable at low stress and high temperatures. Typically this type of process is called pseudoelasticity, since the behavior is such that the material returns to its initial configuration upon removal of the loading. A schematic of this process in the strain-stress space is shown in Figure **1.3**.

Modeling approaches

There are a variety of approaches that have been taken to model and understand the behavior of shape memory alloys. One approach is concerned with describing the process of the phase transformation on a local level. In this approach models are based upon non-convex multi-well free energy functions with the addition of non-local interaction terms to account for interfacial energy at the phase boundaries. Using a Landau-Devonshire based model FALK [1980] applied a multi-well free energy function to describe both stress and thermally induced phase transformations. Additional work along these lines can be found in BALL & JAMES [1992], SUN & HWANG [1993A,B], ABEYARATNE & KNOWLES [1993], KAFKA [1994A,B], ABEYARATNE ET.AL. [1994], KIM & ABEYARATNE [1995], and PATOOR ET. AL. [1996]. Extending these developments MULLER & XU [1991] modeled the characteristics of the phase transformations at high temperatures, specifically pseudoelasticity. Similar in nature are the works of MULLER & WILMANSKI [1981], ACHENBACH & MULLER [1985], ACHENBACH ET. AL. [1986], and ACHENBACH [1989], where arguments from statistical physics have been used to develop a rate-dependent constitutive model to describe the martensitic phase transformation under mechanical and thermal loading. Work *explicitly* examining the computational aspects associated with these types of models does not appear in the literature to the authors' knowledge.

† The symbol σ_{mf} denotes the critical stress above which only martensite is stable.

The significant work done in the area of multi-well models has enabled the development of a phenomenological approach in which the microstructure is accounted for by the introduction of internal variables and the temperature-stress phase space map. TANAKA & IWASAKAI [1985] and TANAKA [1986] utilized the earlier work on free energy functions to develop a rate-independent model which describes the phenomenological behavior of martensitic phase transformations for a one-dimensional bar under a tensile stress state. LIANG & ROGERS [1990] and BRINSON & LAMMERING [1993] were able to build upon this work by creating explicit algebraic evolution equations for the internal variables in conjunction with a phase space diagram; the latter authors also incorporated their model into a finite element setting with finite kinematics for a one-dimensional bar, again restricted to a tensile state of stress. Other numerical work using the internal variable formulation with a phase space diagram in the high temperature regime has been done by AURICCHIO [1995].

Efforts have only recently begun in the area of computational mechanics in regard to general phenomenological shape memory alloy models. The numerical models which have been developed thus far are limited in range of application. To overcome these deficiencies we have developed a one-dimensional constitutive model and algorithm which is applicable to processes from below the martensite finish temperature to above the austenite finish temperature and is good for both tensile and compressive states of stress. The constitutive model is based upon the introduction of internal variables and a phase space map for both tensile and compressive states from which we develop evolution equations which capture the phenomenological behavior of the martensite phase transformations for all temperature and stress states. In addition, an algorithm for state determination is developed which recognizes the possible non-uniqueness of the processes. The issue of state determination, as will been seen, is the most critical aspect of numerical modeling with respect to these materials when they are described by internal variables and a phase space diagram.

The remainder of the paper proceeds as follows. In Section 2 we briefly outline two one-dimensional boundary value problems – a truss bar and a beam. In Section 3 we present the constitutive model. In Section 4 we discuss its integration and in Section 5 we examine several examples.

§2. General Boundary Value Problem

In this section we consider the formulation of a multi-dimensional truss bar and a two dimensional beam element for both linear and nonlinear kinematics. The purpose here is merely set up the problems to be examined and motivate the utility of a one-dimensional constitutive relation.

2.1. Truss Equations.

For the truss examples considered we utilize two types of models: one based entirely on linear kinematics and one based on finite kinematics. The linear case simply assumes that the strain measure is the gradient of the axial displacement of the truss bar. The

expression for the nonlinear strain measure is given by the logarithmic strain measure

$$\varepsilon = \ln\left(\frac{l}{L}\right) \ , \tag{2.1}$$

where L is the initial length and l is the deformed length of the truss bar. In the constitutive equations to be presented later in this paper, the strain measure that appears can be taken to be either Eq. (2.1) or the standard linear measure. The stress measure in both cases can be taken as the Cauchy stress. The governing weak form equations and their finite element approximations are well known and will not be presented here; see e.g. HUGHES [1987] or ZIENKIEWICZ & TAYLOR [1989]. It is noted that in order to solve a finite element truss problem, what is needed is a prescription for computing the element axial stress and tangent given an element strain (in one-dimension).

2.2. Two-dimensional Beam.

For the beam examples given at the end of the paper, the beam formulation of SIMO ET.AL. [1984] is utilized. This formulation assumes that plane sections remain plane, but not necessarily normal after deformation. The strain measures used in this beam are of a full finite deformation character. In the constitutive relation to be presented later in this paper, one can take the stress measure shown to be the axial 2nd Piola-Kirchhoff stress and the strain measure to be the axial component of the Green-Lagrange strain measure. The resultant stress measures for the beam are an axial force, a shear force and a moment. For the problems at hand the shear force is obtained from the penalization of the zero shear strain constraint in thin beams. The axial force and moment are produced by a numerical integration through the thickness of the axial 2nd Piola-Kirchhoff stress. The required resultant tangent is obtained likewise through an integration through the thickness of the variation to the 2nd Piola-Kirchhoff stress measure. Additional details can be found in KASPER [1997].

§3. Constitutive Model

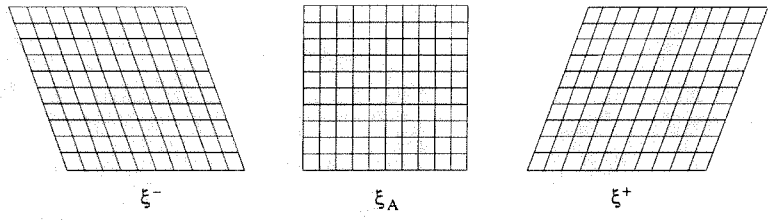

FIGURE 3.1. Conceptual picture of the variants associated with various lattice configurations.

As noted, the boundary value problem for the truss bar and beam is completed by specifying the one-dimensional stress response. Here we assume:

$$\sigma = E\left[\varepsilon - \varepsilon^p - \varepsilon_L\left(\xi^+ - \xi^-\right) - \alpha\left(T - T_0\right)\right] \tag{3.1}$$

where σ is the appropriate stress measure, E is the elastic modulus, ε is the appropriate total strain measure, ε^p is the plastic strain, ε_L is the maximum residual strain obtained by detwinning multiple variant martensite (Bain or transformation strain), ξ^+ and ξ^- are the volume fractions of the positive and negative variants of the martensite twins after ACHENBACH ET.AL. [1986] (see Figure **3.1**), α is the coefficient of thermal expansion and T and T_0 are the current and reference temperatures, respectively.

Remark 3.1.

1. For any state, the simple algebraic relation $\xi^+ + \xi^- + \xi_A = 1$ holds, where ξ_A represents the volume fraction of austenite present. Note that the total martensite fraction is the sum of the variants $\xi = \xi^+ + \xi^-$, while the absence of both ξ^+ and ξ^- indicate the material is completely austenite.
2. For states where $\xi^+ = \xi^-$ the material is considered to be in a self-accommodating state and is termed to be 100% multiple variant martensite. Although its configuration is similar to 100% austenite with regard to the overall deformation, the crystal structure is not the same.
3. For a one-dimensional system we may accurately capture the behavior of the phase transformation using only two internal variables, namely ξ^+ and ξ^-. For higher dimensions, the underlining physics is more complicated and thus additional internal variables or variants are needed; see BOYD & LAGOUDAS [1996A,B].
4. Authors such as TANAKA [1986], LIANG & ROGERS [1990], BRINSON [1993] and BRINSON & LAMMERING [1993] have utilized linear mixture rules for the elastic material modulus $E = E_a + \xi(E_m - E_a)$ and coefficient of thermal expansion $\alpha = \alpha_a + \xi(\alpha_m - \alpha_a)$, where E_a, E_m, α_a and α_m are the elastic moduli and thermal coefficients of expansion for pure austenite and martensite. The mixture rules enhance the model by accounting for different pure state material properties. The addition of these mixtures rules presents no conceptual difficultly in the present formulation; for simplicity we will assume the moduli to be constant. □

In the following subsections, we develop explicit expression for the evolution equations for the martensite fractions for various regions within the phase diagram. To account for both tensile and compressive behavior, we consider a reflection of the standard phase diagram for the tensile stress region onto the compressive region. For the present work, the constitutive transformation parameters are denoted with either a superscript $^+$ or $^-$ representing the parameters in the tensile and compressive regions, respectively. The ability to differentiate between the various transformation parameters enables the model to capture the proper behavior.

3.1. Production of Austenite.

Since austenite has only one form (variant), it is sufficient to consider the evolution of the total martensite fraction. The positive and negative variants are assumed to evolve proportional to the total martensite fraction. Further, the evolution of the total martensite fraction may be expressed in an integrated form as a linear interpolation between the start

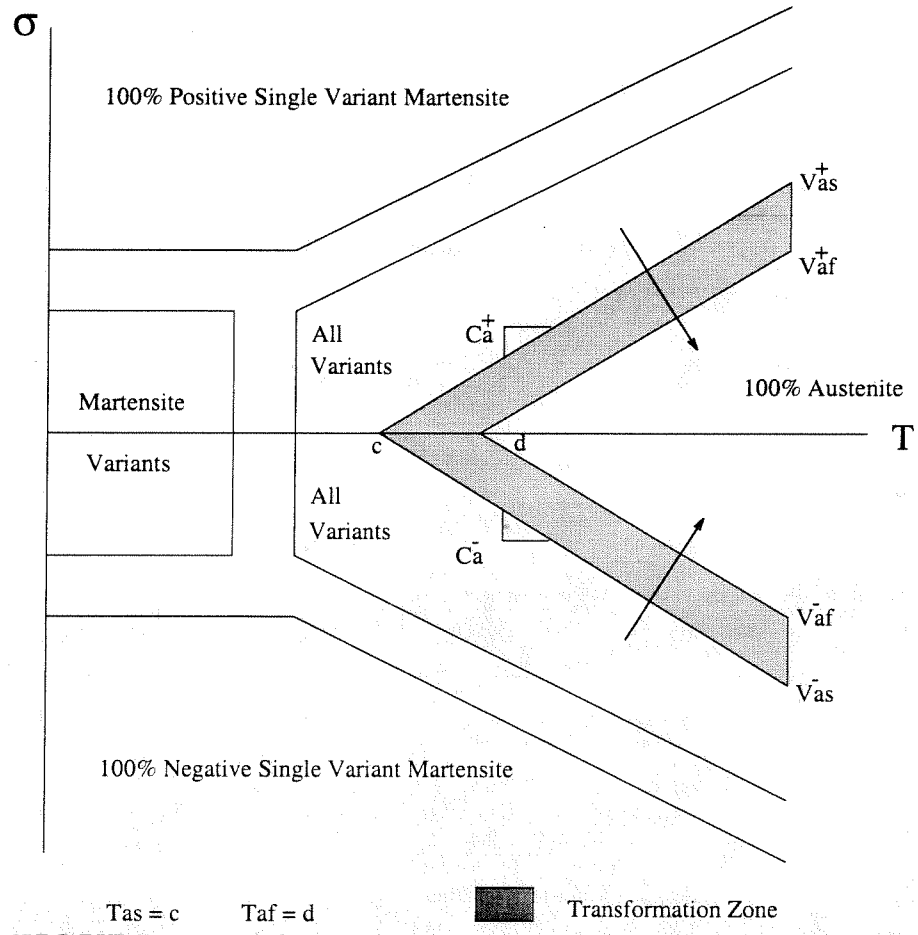

FIGURE 3.2. Admissible transformation regions for the production of austenite. The points 'c' and 'd' denote the start and finish temperatures for the transformation, while $V_{as}^{\pm}$ and $V_{af}^{\pm}$ are the start and finish lines for the transformation; the directionality of the evolution is indicated by the arrows.

and finish transformation lines within the phase transformation region shown in Figure **3.2**.

In the production of austenite from martensite we also consider the effects of plastic deformations. When material in the detwinned (single variant) phase is deformed plastically, the single variant martensite structure becomes "locked in" by the dislocation arrays. This effect prevents the material from subsequently being transformed into austenite or multiple variant martensite; see VANDERMEER ET.AL. [1981], JING-CHEN ET.AL. [1990], and DUTKIEWICZ [1994]. To model this effect, we consider a modification of the usual linear evolution law during this transformation to account for equivalent plastic strain. The evolution equation is expressed as follows:

$$\xi = \xi_p + (1 - f(\bar{\varepsilon}^p) - \xi_p)\left(\frac{\sigma - V_{as}^{\pm}}{V_{af}^{\pm} - V_{as}^{\pm}}\right) . \tag{3.2}$$

In (3.2) $f(\bar{\varepsilon}^p)$ can be interpreted as the maximum amount of austenite that can be pro-

duced for a given equivalent plastic strain. The parameter ξ_p is introduced to account for cyclic behavior within the transformation zone and represents the maximum value of ξ for any previous loading history. The parameters $V_{as}^{\pm}$ and $V_{af}^{\pm}$ denote the critical values of stress between which the phase transformation occurs at a fixed temperature, where the subscripts as and af designate stress values on modified (by the initial conditions) austenite start and finish lines, respectively. The starting value of the phase transformation is taken to be a function of the initial fractions present, while the finish value is taken to be constant; thus

$$\begin{aligned} V_{as}^{\pm} &= \sigma_{as}^{\pm} + \frac{\xi_p - \xi_0}{1 - \xi_0}\left(\sigma_{af}^{\pm} - \sigma_{as}^{\pm}\right) \\ V_{af}^{\pm} &= \sigma_{af}^{\pm}\,, \end{aligned} \tag{3.3}$$

where ξ_0 represents the initial fraction of martensite for the first occurrence of the transformation and $\sigma_{as}^{\pm}$ and $\sigma_{af}^{\pm}$ are defined from the virgin phase transformation lines in the stress-temperature space as

$$\sigma_{as}^{\pm} = C_a^{\pm}\left(T - T_{as}\right) \quad \text{and} \quad \sigma_{af}^{\pm} = C_a^{\pm}\left(T - T_{af}\right) \tag{3.4}$$

and $C_a^{\pm}$ are the slopes of the transformation lines, assumed fixed. The evolution of the positive and negative variants are assumed to occur in proportion to their existence at the beginning of the phase transformation:

$$\xi^{+} = \frac{\xi_p^{+}}{\xi_p}\xi \quad \text{and} \quad \xi^{-} = \frac{\xi_p^{-}}{\xi_p}\xi\,. \tag{3.5}$$

Remark 3.2.

The choice of the superscript ($^+$ or $^-$) depends on whether one transverses the transformation zone with tensile or compressive stresses. Note that the choice is non-trivial since the stress is not known in general *a priori*. This point is discussed in detail in Section 4. □

Remark 3.3.

A suitable two parameter functional form for $f(\bar{\varepsilon}^p)$ is:

$$f(\bar{\varepsilon}^p) = (1 - \beta)\exp[-k\bar{\varepsilon}^p] + \beta\,. \tag{3.6}$$

When there is no plastic strain, equation (3.6) allows for 100% austenite production during the phase transformation. For finite values of $\bar{\varepsilon}^p$, the maximum amount of producible austenite is limited to a value between unity and the asymptotic value of β, taken as a material constant. The rate at which this asymptotic value is approached depends on the material parameter k. For moderate ranges of temperature this model adequately captures the interaction between the plasticity and the shape memory effect. For larger changes in the temperature, considerations such as annealing of the material have to be accounted for; see GOVINDJEE & KASPER [1998] for further details. □

State and Internal Variables

If one assumes that the phase transformation is occurring, then for a given total strain value and temperature the stress and internal variables can be determined by simultaneously solving the constitutive equation (3.1) and the evolution equation for the production of austenite (3.2). Explicitly one has:

$$\begin{aligned} \sigma &= \frac{E}{b_0}\left(\varepsilon - \varepsilon^p - \varepsilon_L[\xi_p^+ - \xi_p^-] + [b_0 - 1]\frac{V_{as}^{\pm}}{E} - \alpha[T - T_0]\right) \\ \xi &= \xi_p + (1 - f(\bar{\varepsilon}^p) - \xi_p)\left(\frac{\sigma - V_{as}^{\pm}}{V_{af}^{\pm} - V_{as}^{\pm}}\right) \end{aligned} \tag{3.7}$$

where

$$b_0 = 1 + \frac{\varepsilon_L E}{\xi_p}\left(\xi_p^+ - \xi_p^-\right)\left(\frac{1 - f - \xi_p}{V_{af}^{\pm} - V_{as}^{\pm}}\right) \ . \tag{3.8}$$

To obtain the mechanical moduli for the inelastic case we take the variation of the stress response $(3.7)_1$. If δ is taken as the variation operator, then:

$$\delta\sigma = \frac{\partial\sigma}{\partial\varepsilon}\delta\varepsilon = \frac{E}{b_0}\delta\varepsilon \ . \tag{3.9}$$

Remark 3.4.

In contrast to the above relations, during an elastic process we would simply have

$$\begin{aligned} \sigma &= E\left(\varepsilon - \varepsilon^p - \varepsilon_L[\xi_p^+ - \xi_p^-] - \alpha[T - T_0]\right) \\ \xi &= \xi_p \ . \end{aligned} \tag{3.10}$$

The tangent would be

$$\delta\sigma = \frac{\partial\sigma}{\partial\varepsilon}\delta\varepsilon = E\delta\varepsilon \ . \tag{3.11}$$

□

3.2. Production of Single Variant Martensites.

For the production of single variant martensites it is sufficient to consider the evolution of one of the variants, either the positive or the negative variant depending on whether the stress state is tensile or compressive. The remaining variant is then evolved proportional to the chosen variant. The evolution of the chosen variant fraction may be expressed in an integrated form as a linear interpolation within the phase transformation zones shown in Figures **3.3** and **3.4**:

$$\xi^{\pm} = 1 + (1 - \xi_p^{\pm})\left(\frac{\sigma - V_{mf}^{\pm}}{V_{mf}^{\pm} - V_{ms}^{\pm}}\right) \ . \tag{3.12}$$

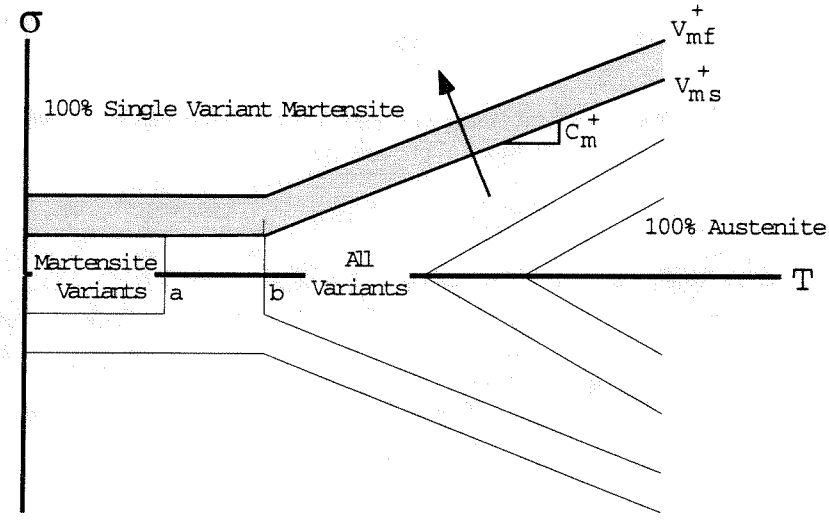

FIGURE 3.3. Admissible transformation regions for the production of positive single variant martensite. The point 'b' denotes the temperature below which austenite is not stable. The parameters V_{ms}^{+} and V_{mf}^{+} are the start and finish lines for the transformation and the directionality of the transformation is indicated by the arrow.

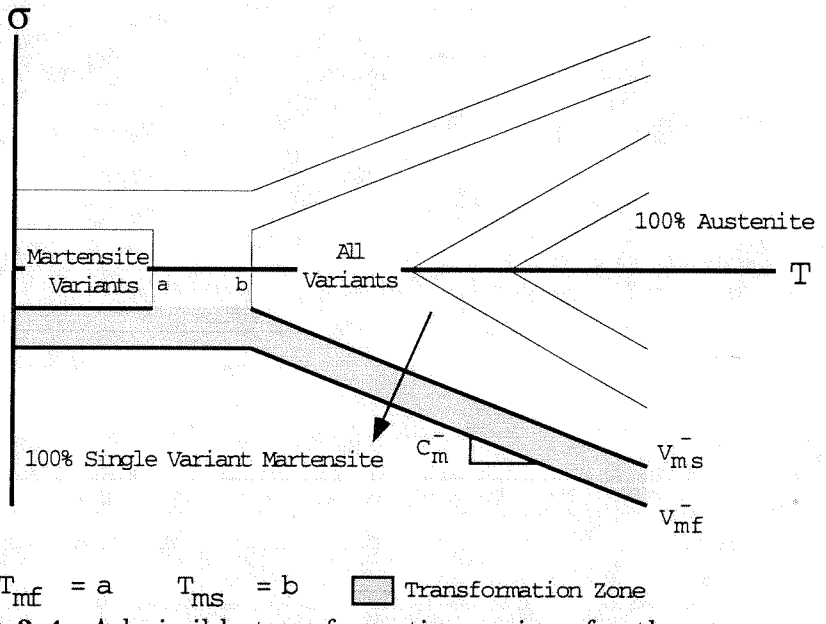

FIGURE 3.4. Admissible transformation regions for the production of negative single variant martensite. The parameters V_{ms}^{-} and V_{mf}^{-} indicate the start and finish lines for the transformation and the direction for the production of negative single variant martensite is depicted by the arrow.

The parameters $\xi_p^{\pm}$ are introduced to account for cyclic behavior within the transformation zones and represent the maximum values of $\xi^{\pm}$ for the previous loading history. The parameters $V_{ms}^{\pm}$ and $V_{mf}^{\pm}$ denote the critical values of stress between which the phase transformations occur at a fixed temperature, where the subscripts ms and mf designate stress values on modified (by the initial conditions) martensite start and finish lines, respectively. The starting value of the phase transformations is taken to be a function of the initial fractions present, while the finish value is taken to be constant; thus

$$\begin{aligned} V_{ms}^{\pm} &= \bar{V}_{ms}^{\pm} + \frac{\xi_p^{\pm} - \xi_0^{\pm}}{1 - \xi_0^{\pm}} \left(V_{mf}^{\pm} - \bar{V}_{ms}^{\pm} \right) \\ V_{mf}^{\pm} &= \sigma_{mf}^{\pm} \\ \bar{V}_{ms}^{\pm} &= \sigma_{ms}^{\pm} + \left(\mathcal{H}(\sigma)\xi_0^{\pm} + [1 - \mathcal{H}(\sigma)]\xi_0^{\mp} - \min[\xi_0^{\pm}, \xi_0^{\mp}] \right) \left(\sigma_{mf}^{\pm} - \sigma_{ms}^{\pm} \right) , \end{aligned} \tag{3.13}$$

where $\xi_0^{\pm}$ represent the initial fraction of martensite for the first occurrence of the transformations, $\mathcal{H}(\sigma)$ is the step function, and $\sigma_{ms}^{\pm}$ and $\sigma_{mf}^{\pm}$ are defined from the virgin phase transformation lines in the stress-temperature space as

$$\sigma_{ms}^{\pm} = \sigma_{cr}^{s\pm} + C_m^{\pm}\langle T - T_{ms} \rangle \quad \text{and} \quad \sigma_{mf}^{\pm} = \sigma_{cr}^{f\pm} + C_m^{\pm}\langle T - T_{ms} \rangle , \tag{3.14}$$

where $\langle \cdot \rangle$ is the Macauley bracket and $C_m^{\pm}$ is the slope of the transformation lines, assumed fixed. The evolution of the remaining variant is assumed to occur in proportion to its existence at the beginning of the phase transformation:

$$\xi^{\mp} = \left(\frac{1 - \xi^{\pm}}{1 - \xi_p^{\pm}} \right) \xi_p^{\mp} . \tag{3.15}$$

Remark 3.5.
In equation $(3.13)_3$ the second term on the right hand side is introduced to ensure that only the single variant states affect the initial critical stress. □

Remark 3.6.
Again, the choice of which transformation is presently occurring for a given strain and temperature can be non-trivial. Section 4 discusses this issue in more detail. □

State and Internal Variables

If as before one assumes that a transformation is occurring with given total strain and temperature, then the constitutive equation (3.1) and the evolution equation for the production of single variant martensite (3.12) may be explicitly solved to determine the stress and martensite fractions during the inelastic process as

$$\begin{aligned} \sigma &= \frac{E}{b_0} \left(\varepsilon - \varepsilon^p - \varepsilon_L + (b_0 - 1)\frac{V_{mf}^{\pm}}{E} - \alpha[T - T_0] \right) \\ \xi^{\pm} &= 1 + (1 - \xi_p^{\pm}) \left(\frac{\sigma - V_{mf}^{\pm}}{V_{mf}^{\pm} - V_{ms}^{\pm}} \right) \end{aligned} \tag{3.16}$$

where

$$b_0 = 1 + \varepsilon_L E \left(\frac{1 - \xi_p^{\pm} + \xi_p^{\mp}}{V_{mf}^{\pm} - V_{ms}^{\pm}} \right) . \tag{3.17}$$

The tangent for the inelastic case is given by the variation of the stress response $(3.16)_1$ as:

$$\delta\sigma = \frac{\partial\sigma}{\partial\varepsilon}\delta\varepsilon = \frac{E}{b_0}\delta\varepsilon . \tag{3.18}$$

3.3. Production of Multiple Variant Martensite.

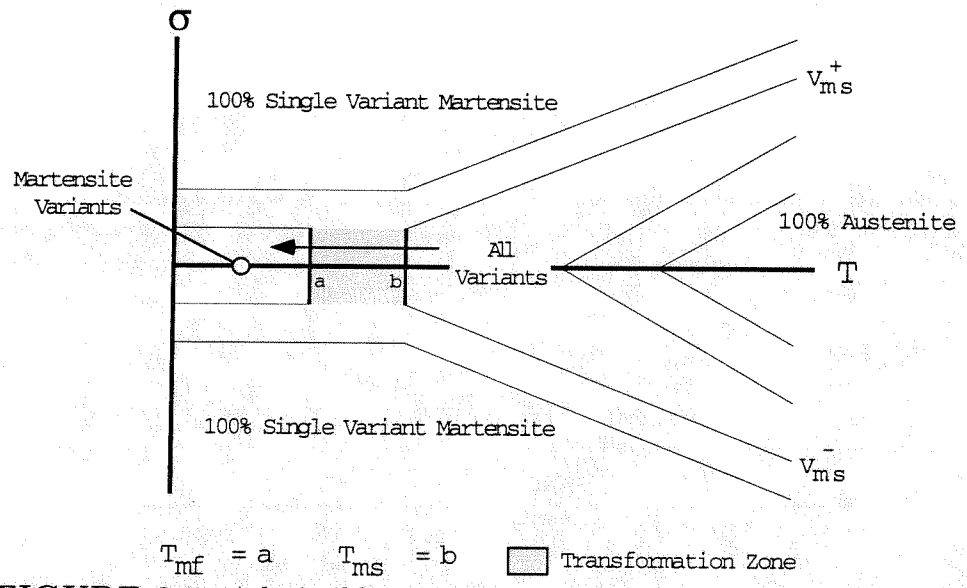

FIGURE 3.5. Admissible transformation regions for the production of multiple variant martensite. The points 'a' and 'b' denote the start and finish temperatures for the phase transformation; the direction of the evolution is depicted by the arrow.

Since multiple variant martensite is produced in equally distributed proportions of positive and negative variants, from a zero initial state†, it is sufficient to consider the evolution of the total martensite fraction. The positive and negative variants are then evolved proportional to the total martensite fraction present. In an integrated form, this evolution may be expressed as a linear interpolation within the phase transformation zone shown in Figure **3.5**:

$$\xi = 1 + (1 - \xi_p) \left(\frac{T - \theta_{mf}}{\theta_{mf} - \theta_{ms}} \right) . \tag{3.19}$$

Again the parameter ξ_p is introduced to account for cyclic behavior within the transformation zone and represents the maximum value of ξ for the previous loading history. The parameters θ_{ms} and θ_{mf} denote the critical values of temperature between which the phase

† Producing multiple variant martensite from 100 % austenite.

transformation occurs, where the subscripts ms and mf designate temperature values on modified (by the initial conditions) martensite start and finish lines, respectively. The starting value of the phase transformation is taken to be a function of the initial fractions present, while the finish value is taken to be constant; thus

$$\begin{aligned} \theta_{ms} &= T_{ms} + \frac{\xi_p - \xi_0}{1 - \xi_0}\,(T_{mf} - T_{ms}) \\ \theta_{mf} &= T_{mf} \end{aligned} \tag{3.20}$$

where ξ_0 represents the initial fraction of martensite for the first occurrence of the transformation and T_{ms} and T_{mf} are material parameters taken from the virgin phase transformation lines in the stress-temperature space.

The evolution of the positive and negative variants are assumed to occur in proportion to their existence at the beginning of the phase transformation

$$\xi^+ = \xi_p^+ + \frac{1}{2}(\xi - \xi_p) \quad \text{and} \quad \xi^- = \xi_p^- + \frac{1}{2}(\xi - \xi_p)\ . \tag{3.21}$$

State and Internal Variables

During this phase transformation one can solve for the stress and internal variables given the total strain and temperature by first noting that the evolution equation for the production of multiple variant martensite (3.19) is independent of the constitutive equation (3.1). Hence one may simply calculate the martensite fractions (assuming a known temperature) from Eqs. (3.19)-(3.21) and substitute these values into the constitutive equation (3.1) to get the stress. The variation of the the stress response gives the elastic modulus for the tangent.

3.4. Plasticity.

To account for the behavior of the material at high values of stress we utilize a linear isotropic hardening model and assume that the evolution of the plastic variables occurs independent of any phase transformations. Hence, the plasticity model described below is not intended for use at high temperatures where transformations occur at high stress. (Note adequate experimental data does not exist in this regime, thus modeling is unrealistic.)

The internal variables used for the plasticity model are plastic strain and equivalent plastic strain and their evolution is given by

$$\begin{aligned} \dot{\varepsilon}^p &= \lambda \text{sign}\,[\sigma] \\ \dot{\bar{\varepsilon}}^p &= \lambda \end{aligned} \tag{3.22}$$

where λ is the plastic consistency parameter and the yield function is defined as

$$\phi(\sigma, \bar{\varepsilon}^p) = |\sigma| - (\sigma_y + H\bar{\varepsilon}^p)\,, \tag{3.23}$$

where σ_y is the uniaxial yield stress, H the isotropic hardening modulus and the Kuhn-Tucker conditions are given as

$$\phi \le 0; \quad \lambda \ge 0; \quad \lambda\phi = 0; \quad \lambda\dot{\phi} = 0. \tag{3.24}$$

For further details on the plasticity portion of our model see SIMO & HUGHES [1998].

§4. Integration and State Determination

This section covers the algorithmic approximation of the constitutive theory in the setting of the finite element method and the integration pathologies which arise. In particular we restrict ourselves to a single Gauss point and assume the state of the material is known at time t_n. The solution is to be advanced to a new time t_{n+1} and the temperature and strain are assumed given to the constitutive routine by the general FEM machinery with the goal being to compute the stress, material tangent, and internal variables. Due to the nature of the nested elastic and inelastic regions, the determination of the activation of a transformation is paramount to the model's implementation. This detection procedure is known as state determination and although seemingly straight-forward has several subtleties, which if not accounted for can lead to global convergence problems. Note that the stress is not known; thus one's position of the phase space diagram is unknown.

There are two basic pathologies that must be treated. First, when considering an individual transformation three possible events can occur (a) elastic "unloading" with no change in the internal variables, (b) forward transformation with evolution of the internal variables as specified in the previous sections, and (c) completion of the transformation with the evolution of the internal variables restricted by the physical phase fraction limits. In terms of the evolution equations for the internal variables, this actually makes them piecewise linear in the stress-internal variable space with three "branches". When computing the intersection of this piecewise linear evolution equation and the constitutive relation (3.1) it is possible to have multiple intersections, e.g. multiple admissible states. The primary algorithmic issue then is the "state determination" – i.e. which of the three possibilities is the correct one. This non-uniqueness is termed an intra-transformation pathology. Below we propose a heuristic for making the seemingly correct determination among the three possible choices. The second pathology that must be considered is that at any given temperature and strain increment there are multiple types of transformations possible; e.g. if $T > T_{af}$, then one can have the production of positive single variant martensite, the generation of austenite from above or below the zero stress axis, and the production of negative single variant martensite. It is possible for a given history, temperature, and strain increment to have three of these as valid possibilities. This non-uniqueness is termed an inter-transformation pathology. Here too we propose a simple heuristic that allows us to choose the seemingly correct transformation path.

4.1. Intra-transformational Pathology.

Production of Austenite

Consider the production of austenite with initial conditions at time t_n shown in Figure **4.1**. Given a temperature increase to T_{n+1} and a strain increment to ε_{n+1} we wish to determine the state for time t_{n+1}. In Figure **4.1** (b) the abscissa is the total martensite fraction that is decreasing from its current value ξ_n to zero by an increase in the system temperature. If at time t_{n+1} the stress σ_{n+1} is above σ_2, then the transformation is completed and ξ_n equals zero. If on the other hand $\sigma_2 > \sigma_{n+1} > \sigma_1$, then the transformation takes place partially and the value of ξ_{n+1} is given as in Section 3. If $\sigma_{n+1} < \sigma_1$ then

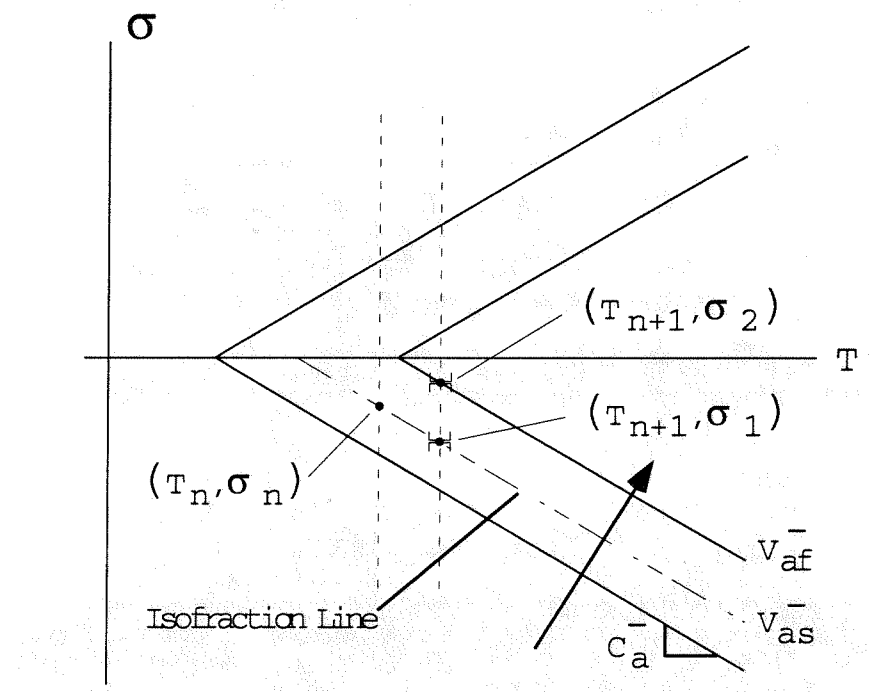

(a)

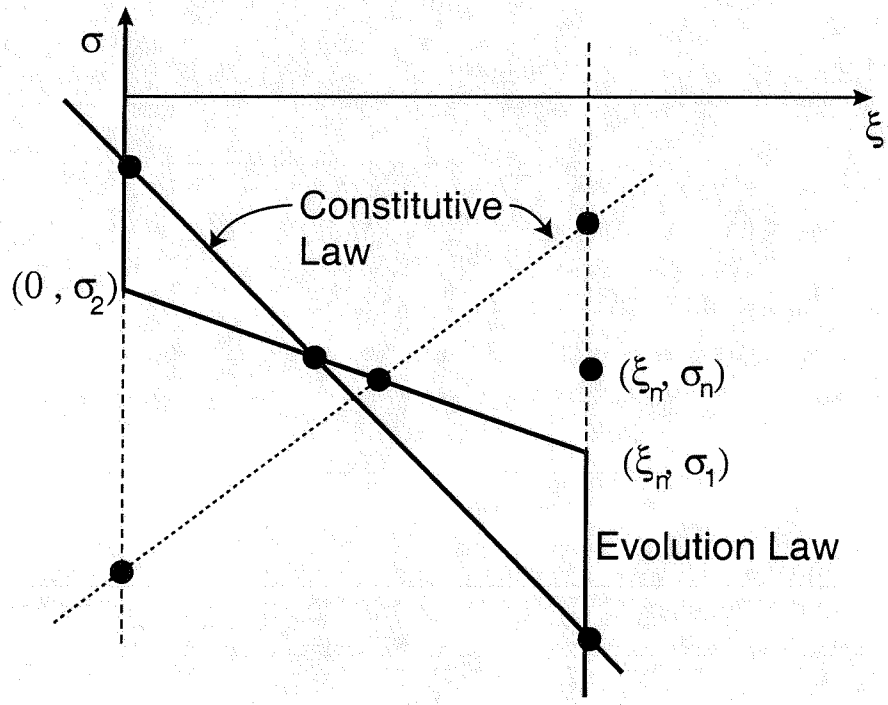

(b)

FIGURE 4.1. Production of austenite. (a) phase space diagram of initial state at time t_n and possible final states at time t_{n+1} and temperature T_{n+1}. (b) piecewise linear evolution law and two cases for the constitutive relation (3.1).

$\xi_{n+1} = \xi_n$ and an elastic "unloading" takes place. Also shown in Figure **4.1** (b) is equation (3.1); it is shown for two cases – one where $\xi_n^+ > \xi_n^-$ and the other for $\xi_n^- > \xi_n^+$. The difference between the two cases changes the slope and thus the intersection characteristics of (3.1) with the evolution law (also shown in Figure **4.1** (b) as the piecewise linear curve). For the case of a negative slope, three constitutively consistent possibilities can arise.

To algorithmically determine the correct solution the three cases above (elastic unload, partial transformation, and complete transformation) are each assumed correct and evaluated. Next consistency checks are performed:

- For the elastic case if the stress is less than the value of the stress at the iso-fraction line for $\xi = \xi_n$ at $T = T_{n+1}$ $(\sigma < \sigma_1)$ then the path is admissible.
- For the partial transformation case if the stress is less than the value of the stress at the iso-fraction line for $\xi = \xi_{apex} = \max\left\{\xi_0 + (1 - f - \xi_0)\frac{\langle T - T_{as}\rangle}{T_{af} - T_{as}}, 0\right\}$ at $T = T_{n+1}$ $(\sigma < \sigma_2)$ and greater than the value of the stress at the iso-fraction line for $\xi = \xi_n$ at $T = T_{n+1}$ $(\sigma > \sigma_1)$ then the path is admissible.
- For the complete transformation case if the stress is greater than the value of the stress at the iso-fraction line for $\xi = \xi_{apex}$ at $T = T_{n+1}$ $(\sigma > \sigma_2)$ then the path is admissible.

If no paths are found admissible, then this transformation is inactive. If only one path is found admissible it is taken as active. If multiple paths are found to be admissible, as depicted in the stress-fraction map in Figure **4.1** (b) then the trajectory which minimizes the phase space norm $d(\sigma_n, \sigma_i)$ is chosen as active. Minimizing the distance in phase space aids in controlling the local behavior of the constitution. Note that an active path may not be the actual path due to inter-transformational pathologies.

Production of Positive Single Variant Martensite

Consider now the production of positive single variant martensite with initial conditions at time t_n shown in Figure **4.2**. Given a temperature increase to T_{n+1} we wish to determine the state for time t_{n+1}. From the stress-phase fraction map in Figure **4.2** (b) we see that there are three branches to the evolution equation, viz.

- An elastic unload branch in which the stress is below the iso-fraction line $\xi^+ = \xi_n^+$ $(\sigma < \sigma_1)$ in phase space. For this path the internal variables remain constant.
- A partial transformation branch in which positive single variant martensite is produced if the state of stress is above the iso-fraction line $\xi^+ = \xi_n^+$ at $T = T_{n+1}$ $(\sigma > \sigma_1)$ and below the completion line V_{mf}^+ $(\sigma < \sigma_2)$. For this trajectory both the stress and the internal variable are computed via the constitution as in Section 3.
- A complete transformation branch in which the internal variable $\xi^+ = 1$ with the final state $(\sigma > \sigma_2)$.

To determine which, if any, of these paths are admissible the three cases are evaluated assuming they are each active. Next consistency checks are performed:

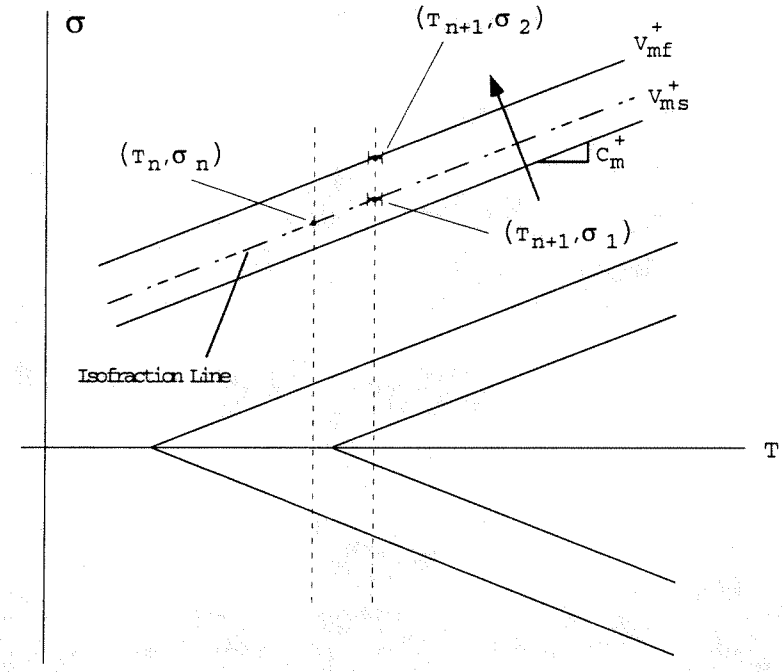

(a)

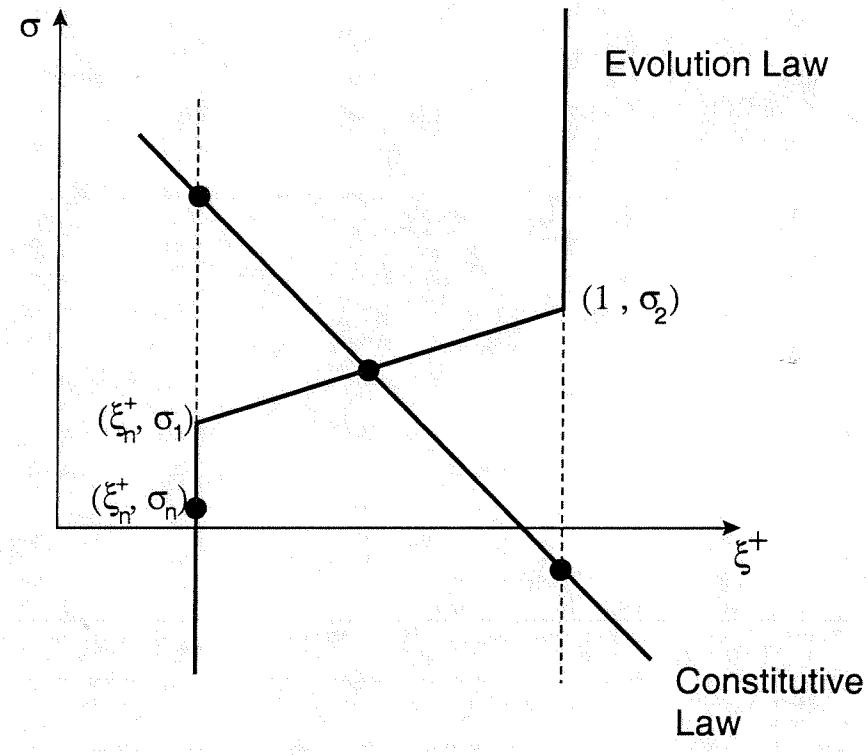

(b)

FIGURE 4.2. Production of positive single variant martensite. (a) phase space diagram of initial state at time t_n and possible final states at time t_{n+1} and temperature T_{n+1}. (b) piecewise linear evolution law and the constitutive relation (3.1).

- For the elastic unload case if the stress $\sigma_{n+1} < \sigma_1$ then the path is admissible.
- For the partial transformation case if the stress $\sigma_1 < \sigma_{n+1} < \sigma_2$ then the path is admissible.
- For the complete transformation case if the stress $\sigma_{n+1} > \sigma_2$ then the path is admissible.

Although not shown in the stress-fraction map in Figure **4.2** (b) multiple admissible paths may arise if $\xi_n^+ < \xi_n^-$. If multiple paths are found then the phase space norm is utilized to determine which path is chosen.

Remark 4.1.

1. An identical situation exists with respect to the creation of negative single variant martensite and it can be treated in a similar manner.
2. For multiple variant martensite production, pathologies of the type being delineated do not exist since the constitutive relation (3.1) is decoupled from the phase fraction evolution. The only consideration is that one cannot produce more than 100% martensite. □

4.2. Inter-transformational Pathology.

The inter-transformational pathology can most easily be appreciated by looking at a specific example. Consider the case shown in Figure **4.3**, where at time t_n the phase fractions are assumed to be given by $\xi_n^+ = 0$ and $\xi_n^- = 1$. Further, consider an increment in the temperature to above T_{af} as shown. In the FEM solution procedure a value of strain will be passed to the constitutive routine and the stress, material tangent, and phase fractions will need to be computed. Consider for concreteness the possible partial generation of austenite via a path below the zero stress axis, one above the axis, and the possible generation of positive single variant martensite. It can be shown that a given value of strain can be compatible with all of these transformation paths. Using Eq. (3.1), one can show that if

$$\varepsilon_{n+1} \in \left(\frac{V_{af}^-}{E} + \alpha\Delta T + \varepsilon^p, \frac{V_{as}^-}{E} + \varepsilon_L + \alpha\Delta T + \varepsilon^p\right), \tag{4.1}$$

then one has an admissible partial production of austenite that results in a negative value for the stress, $V_{as}^- < \sigma_{n+1} < V_{af}^-$. Further, also using (3.1), if

$$\varepsilon_{n+1} \in \left(\frac{V_{af}^+}{E} + \alpha\Delta T + \varepsilon^p, \frac{V_{as}^+}{E} + \varepsilon_L + \alpha\Delta T + \varepsilon^p\right), \tag{4.2}$$

then one has an admissible partial production of austenite that results in a positive value for the stress, $V_{af}^+ < \sigma_{n+1} < V_{as}^+$. Again, using (3.1), if

$$\varepsilon_{n+1} \in \left(\frac{V_{ms}^+}{E} + \alpha\Delta T + \varepsilon^p, \frac{V_{mf}^+}{E} + \varepsilon_L + \alpha\Delta T + \varepsilon^p\right), \tag{4.3}$$

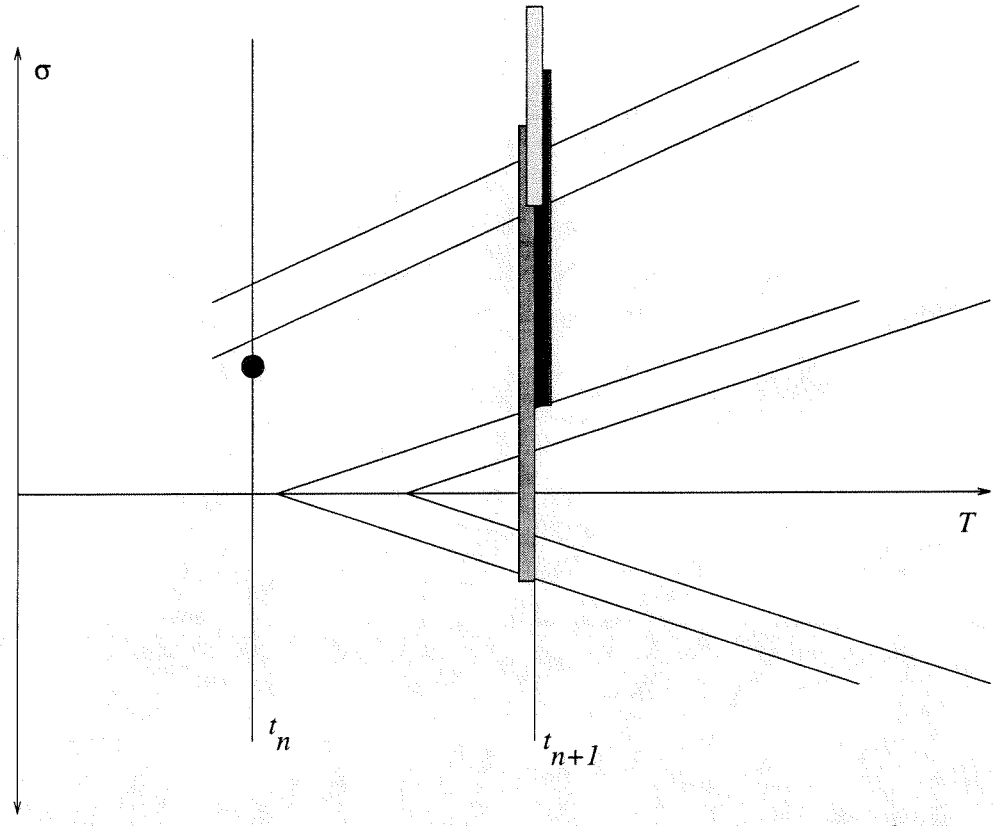

FIGURE 4.3. An example of an inter-transformational integration pathology when $\xi_n^+ < \xi_n^-$. Shaded zones indicate trial stress values that produce nominally admissible partial transformations; light-bar – production of positive single variant martensite, med-bar – production of austenite with negative stresses, dark-bar – production of austenite with positive stresses.

then one has an admissible partial production of positive single variant martensite that results in a positive value for the stress, $V_{ms}^+ < \sigma_{n+1} < V_{mf}^+$. The three strain ranges given can easily overlap each other leading to multiple admissible transformations of differing types – i.e. an inter-transformational pathology or non-uniqueness in the constitution.

Remark 4.2.

Consider for instance: $V_{as}^+ = -V_{as}^- = 100$, $V_{af}^+ = -V_{af}^- = 50$, $V_{ms}^+ = 200$, $V_{mf}^+ = 250$, $\alpha = 0$, $\varepsilon^p = 0$, $\varepsilon_L = 0.05$, and $E = 100 \times 10^3$. Then the three ranges given above for the strain at time t_{n+1} are $(-0.5, 49.0)$, $(0.5, 51.0)$, and $(2, 52.5)$ milli-strain, respectively. The regions clearly overlap □

Remark 4.3.

A useful pictorial representation is given in Figure **4.3**, where the strain ranges have been converted to "trial-stress" values. In other words the end points of the strain ranges have been used to compute stresses from the constitutive relation (3.1) with the phase fractions fixed at the t_n values. Trial stress values falling on a particular shaded

bar will result in an admissible partial transformation of a particular type. The lightest bar is for positive single variant martensite production, the intermediately shaded bar is for austenite production with negative stresses and the darkest bar is for austenite production with positive stresses. □

Once all possible transformation zones have been computed for a given temperature state and the individual intra-transformation non-uniquenesses treated, an inter-transformational check is performed to determine which transformation is admissible. To perform this check the mixture energy is computed for all admissible transformations and the path which yields the minimum mixture energy is chosen as the state for the current iteration:

$$\min_k \Pi_k = \xi_k^- \tfrac{1}{2} E(\varepsilon + \varepsilon_L)^2 + \xi_k^+ \tfrac{1}{2} E(\varepsilon - \varepsilon_L)^2 + (1 - \xi_k^+ - \xi_k^-) \tfrac{1}{2} E\varepsilon^2 \,. \tag{4.4}$$

The combination of these two simple heuristics provides the "desired" constitutive behavior in a *robust* fashion.

§5. Numerical Simulations

In this section we consider the application of the proposed model and algorithm to several test cases. In particular we consider 3 isothermal processes ($T < T_{mf}$, $T_{as} < T < T_{af}$, and $T > T_{af}$) and one shape memory cycle. The material under consideration will be a Nickel-Titanium alloy whose relevant properties are listed in Table 1. For examples involving plasticity, the reader is referred to GOVINDJEE & KASPER [1998]. All the examples shown will involve spatially inhomogeneous states of deformation and involve partial transformations at certain spatial locations.

Table 1: Material Properties for NiTi.(BRINSON & LAMMERING [1993])

Young's Moduli $E_m = E_a = 67$ GPa
Critical stresses for de-twinning $\sigma_{cr}^{s\pm} = \pm 100$ MPa and $\sigma_{cr}^{f\pm} = \pm 170$ MPa
Martensite production temperatures $T_{ms} = 18.4$ C and $T_{mf} = 9$ C
Austenite production temperatures $T_{as} = 34.5$ C and $T_{af} = 49$ C
Austenite production slope $C_a^{\pm} = \pm 13.8$ MPa/C
Martensite production slope $C_m^{\pm} = \pm 8$ MPa/C
Maximum transformation strain $\varepsilon_L = 0.067$
Thermal expansion coefficient $\alpha = 6.5$ μstrain/C

5.1. NiTi Truss-Bridge Under Cyclic Loading.

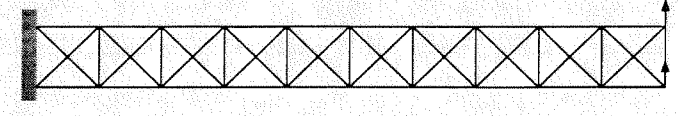

FIGURE 5.1. Reference configuration for the truss-bridge.

We consider a NiTi cantilever truss-bridge consisting of 53 elements shown in Figure **5.1**. The bridge is 20 (m) long by 2 (m) deep and all elements have an initial area $\Omega_0 = 1$ (m^2). Two simulations are performed to demonstrate the ability of the algorithm to predict the behavior of a system with spatial inhomogeneities for $T < T_{mf}$ and in a shape memory cycle.

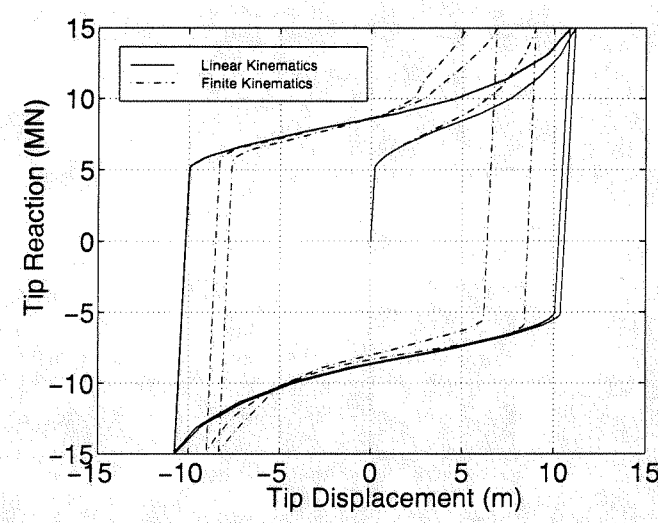

FIGURE 5.2. Simulation # 1: Response curves for isothermal conditions at 5 C for both linear and finite kinematics.

Simulation #1

The truss-bridge is isothermally cycled to a peak load of ± 15 MN at a temperature of 5 C. The initial state of the material is 100% multiple variant martensite (i.e. $\xi_0^+ = \xi_0^- = 0.5$). The response curve at the tip is shown in Figure **5.2**.

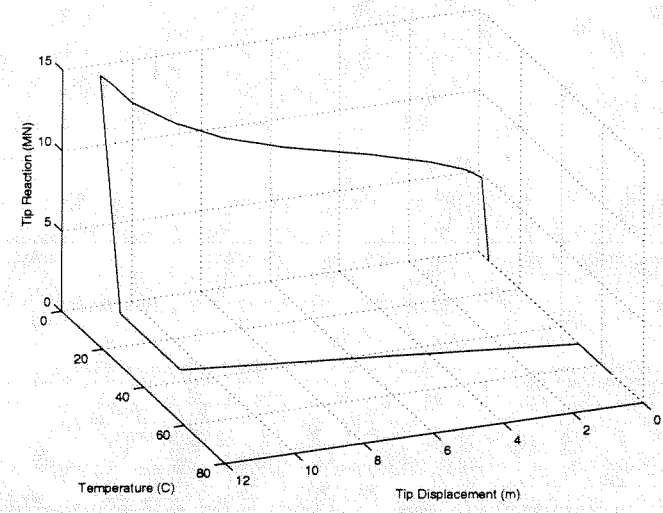

FIGURE 5.3. Simulation # 2: Thermo-mechanical response curve for linear kinematics.

Simulation #2

The truss-bridge is isothermally loaded at a temperature of 5 C to a peak load of 15 MN and then unloaded. The initial state of the material is 100% multiple variant martensite (i.e. $\xi_0^+ = \xi_0^- = 0.5$). The truss-beam is then heated to 65 C to facilitate the recovery of the residual strain incurred during the mechanical loading stage. The response curve at the tip is shown in Figure **5.3**.

Remark 5.1.

1. The algorithm is seen to accurately reproduce the global response of the system that would be expected for these two load cycles.
2. The ability of the algorithm to robustly handle these problems stems from the complete state determination algorithm employed. It is noted that the spatially inhomogeneous nature of these examples makes them much more challenging than the corresponding loading applied to a single truss bar. In the single truss bar case, the interaction with the boundary value problem is non-existent and one is simply integrating the constitutive relations. In the spatially inhomogeneous case, the algorithm is also dealing with a wide variety of trial strain increments which may be far from the actual solution.
3. For simulation #1 we see that there exists a global evolution in the response. This evolution is a result of the fractions changing differing amounts in various bars. These oscillations reach a limit cycle in a few load cycles and repeatability of the response is then seen. □

5.2. NiTi Beam Under Cyclic Loading.

We now consider a ten element discretization of a NiTi cantilever beam of length $L = 20$ (m) having a rectangular cross section of 2×1 (m^2). The cross section is divided into four layers, each of which is evaluated using a 5-pt Gauss-Lobatto quadrature rule. Standard 1-pt Gaussian quadrature was used along the axis of each element. The beam is fixed against translations and rotations on the one end ($X_1 = 0$) and loaded via displacement control in the X_2 (vertical) direction at the other end ($X_1 = L$).

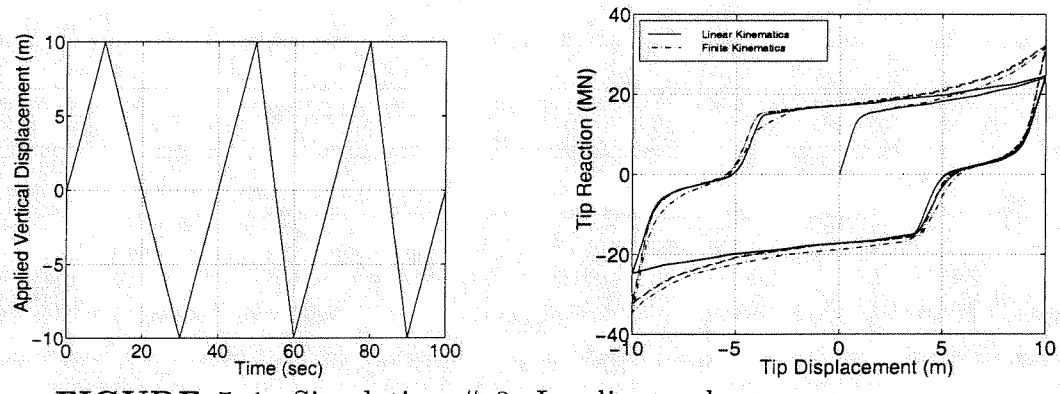

FIGURE 5.4. Simulation # 3: Loading and response curves for both linear and finite kinematics.

Simulation #3

The temperature of the beam is held constant at $T = 41.75$ C, which is above the austenite start temperature and below the austenite finish temperature. The initial state is assumed to be 50% multiple variant martensite (i.e. $\xi_0^+ = \xi_0^- = 0.25$) and the loading and response curves are shown in Figure **5.4**.

Remark 5.2.

1. The algorithm accurately determines the onset and completion of negative and positive martensitic phase transformations for each quadrature point through the depth of the beam resulting in a behavior which is qualitatively correct.
2. The model predicts the termination of an austenite transformation when the net reaction is zero. This produces the kinked response curves.
3. Although the strain levels within the beam are moderate the rotations are large and their effects are pronounced as can be seen from the different response curves for the linear and finite kinematics. □

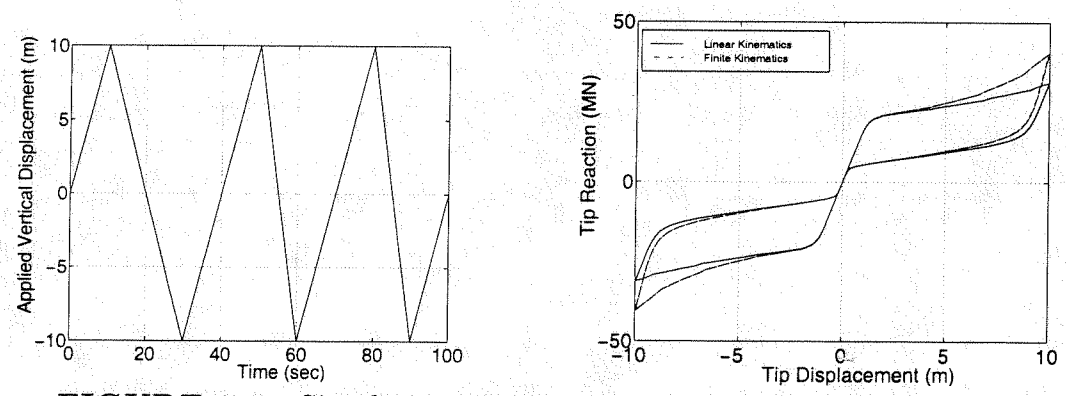

FIGURE 5.5. Simulation #4: Loading and response curves for both linear and finite kinematics.

Simulation #4

Here the temperature of the beam is held constant at $T = 55$ C, which is above the austenite finish temperature. The initial state is assumed to be 100% austenite (i.e. $\xi_0^+ = \xi_0^- = 0$) and the loading and response curve are shown in the Figure **5.5**.

Remark 5.3.

1. As before one can see that the algorithm correctly reproduces the expected response curve.
2. From the experimental data shown in AURICCHIO ET.AL. [1995] the model is seen to qualitatively captures the essential behavior of the pseudoelastic effect.

3. Since the beam has multiple quadrature points through the depth it provides a rigorous examination of the algorithm, due to the existence of highly complex through thickness stress states. □

§6. Closure

This paper has addressed constitutive modeling of one-dimensional shape memory alloys from the perspective of the phase space map. The constitutive model developed with its associated evolution equations were cast within a finite element setting for a truss bar and beam element. The model, although limited to one-dimensional behavior, encompasses nearly all devices and components currently in use. Further, we can remark that:

1. The macroscopic behavior of the model accurately captures the essential features of the actual response of shape memory alloys such as Nickel-Titanium.
2. Complex loading and unloading paths are taken into account via a robust algorithm which determines the active state and associated evolutionary equations for nested elastic and inelastic zones in stress-temperature space.
3. While not shown explicitly in the example section, the simulations can be run with time steps so large as to actually jump over transformation zones in the phase space. This type of robustness permits the rapid computation of highly complex beam and truss systems. This is a feature of the phase space model that makes it very attractive in the 1-D setting.
4. It is noted, however, that the extension of phase space models to multi-dimensions possesses several hurdles that are difficult to overcome. Thus, in multi-dimensions, multi-well models appear to be the only viable modeling avenue. Robust integration methods for such models will be of great interest.
5. The pathologies noted are due to the fact that we have considered the affects of compressive and tensile stresses simultaneously. Previous models were restricted to only tensile states and thus these pathologies did not arise. The consideration of the complete stress range brings these issues to the surface.

§7. References

ABEYARATNE, R., KIM, S-J. & KNOWLES, J.K. [1994], "Continuum Modeling of Shape-Memory Alloys", *ASME International Congress and Exposition*, Chicago, ASME, Proceedings of the Symposium on Phase Transformations and Shape Memory Alloys, AMD-Vol 189, L.C. Brinson & B. Moran Eds. : 59-69.

ABEYARATNE, R. & KNOWLES, J.K. [1993], "A continuum model of a thermoelastic solid capable of undergoing phase transitions", *J. Mech. Phy. Solids*, **41**: 541-571.

ACHENBACH, M. & MULLER, I. [1985], "Simulation of Material Behavior of Alloys with Shape Memory", *Arch. Mech.*, **35** : 537-585.

ACHENBACH, M. [1989], "A Model for an Alloy with Shape Memory", *Int. J. Plast.*, **5**: 371-395.

ACHENBACH, M., ATANACKOVIC, T. & MULLER, I. [1986], "A Model for Memory Alloys in Plane Strain", *Int. J. of Solids & Struct.*, **22** : 171-193.

AURICCHIO, F. [1995], "Shape Memory Alloys: applications, micromechanics, macromodeling and numerical simulations", Ph.D. dissertation, University of California at Berkeley, Department of Civil Engineering.

BALL, J.M. & JAMES, R.D., [1992], "Proposed Experimental Tests of a Theory of Fine Microstructure and the 2-well Problem", *Philosophical Transactions of the Royal Society of London Series A-Physical Sciences and Engineering*, **338**: 389-450.

BOYD, J.G. & LAGOUDAS, D.C. [1996A], "A Thermodynamic Constitutive Model for the Shape Memory Materials. Part I. The Monolithic Shape Memory Alloy", *Int. J. Plast.*, **12** 805-842.

BOYD, J.G. & LAGOUDAS, D.C. [1996B], "A Thermodynamic Constitutive Model for the Shape Memory Materials. Part II. The SMA Composite Material", *Int. J. Plast.*, **12** 843-873.

BRINSON, L.C. [1993], "One Dimensional Constitutive Behavior of Shape Memory Alloys: Thermomechanical Derivation with Non-Constant Material Functions", *J. Intell. Matl. Syst. & Struct.*, **4**: 229-242.

BRINSON, L.C. & LAMMERING, R. [1993], "Finite Element Analysis of the Behavior of Shape Memory Alloys and their Applications", *Int. J. Solids & Struct.*, **30**: 3261-3280.

DUERIG, T.W., MELTON, K.N., STOCKEL, D. & WAYMAN, C.M. [1990], *Engineering Aspects of Shape Memory Alloys* , Butterworth-Heinemann, Boston.

DUTKIEWICZ, J., [1994], "PLASTIC DEFORMATION OF CUALMN SHAPE-MEMORY ALLOYS", *J. Mat. Sci.*, **29**: 6249-6254

FALK, F. [1980], "Model Free Energy, Mechanics, and Thermodynamics of Shape Memory Alloys", *Acta Metall.*, **28**: 1773-1780.

FUNAKUBO, H., [1984] *Shape Memory Alloys*, Translated by: J.B. Kennedy, Gordon and Breach Science Publishers.

GOVINDJEE, S. & KASPER, E.P. [1998], "A Shape Memory Model for Uranium-Niobium Accounting for Plasticity", *J. Intell. Mat. Sys. Struct.* (in press).

HUGHES [1987], *The Finite Element Method*, Prentice-Hall, Englewood Cliff, N.J.

JING-CHENG, W., ZI-CHANG, S., HAO, Z., AND HAI-JING, W., [1990], "An Anomaly of the Parameters of Positron Annihilation for Plastically Deforming Shape Memory Alloys," *Scipta Metallurgica et Materialia*, **24**: 1511-1513.

KAFKA, V. [1994A], "Shape Memory: A New Concept of Explanation and Mathematical Modeling. Part I: Micromechanical Explanation of the Causality in the SM Processes", *J. Intell. Matl. Syst. & Struct.*, **5**: 809-814.

KAFKA, V. [1994B], "Shape Memory: A New Concept of Explanation and Mathematical Modeling. Part II: Mathematical Modeling of the SM Effect and of Pseudoelasticity", *J. Intell. Matl. Syst. & Struct.*, **5**: 815-824.

KASPER, E.P. [1997], "Shape Memory Materials: Constitutive Modeling and Finite Element Analysis," Ph.D. Dissertation, Univeristy of California at Berkeley, Berkeley, CA.

KIM, S-J. & ABEYARATNE, R. [1995], "On the Effect of the Heat Generated During a Stress Induced Thermoelastic Phase Transformation", *Continuum Mechanics & Thermodynamics*, **7**: 311-332.

LIANG, C. & ROGERS, C.A. [1990], "One-Dimensional Thermomechanical Constitutive Relations for Shape Memory Materials", *J. Intell. Matl. Syst. & Struct.*, **1**: 207-234.

MULLER, I. & XU, H. [1991], "On the pseudo-elastic hysteresis", *Acta Metall.*, **39**: 263-271.

MULLER, I. & WILMANSKI, K. [1981], "Memory Alloys, Phenomenology and Ersatz Model", in Brulin, O., Hsieh, R.K.T. (eds.), *Continuum Models of Discrete Systems*, **4**, North Holland Pub. Co.

PATOOR, E., EBERHARDT, A & BERVEILLER, M. [1996], "Micromechanical Modeling of Superelasticity in Shape Memory Alloys", *J. Physique III*, International Conference on Martensitic Transformation, ICOMAT 95 Part II,Vol **6**, Colloque C1:277.

SIMO, J.C., HJELMSTAD, K.D. & TAYLOR, R.L. "Numerical Formulations of Elasto-viscoplastic Response of Beams Accounting for the Effect of Shear", *Comput. Methods Appl. Mech. Engrg.*, **42**: 301-330.

SIMO, J.C. AND HUGHES, T.J.R. *Elastoplasticity and Viscoplasticity: Computational Aspects*, Springer-Verlag, (to appear 1998).

SUN, Q.P. & HWANG, K.C. [1993A], "Micromechanics Modeling for the Constitutive Behavior of Polycrystalline Shape Memory Alloys - I. Derivation of General Relations", *J. Mech. Phys. Solids*, **41**: 1.

SUN, Q.P. & HWANG, K.C. [1993B], "Micromechanics Modeling for the Constitutive Behavior of Polycrystalline Shape Memory Alloys - II. Study of the Individual Phenomena", *J. Mech. Phys. Solids*, **41**: 19.

TANAKA, K. & IWASAKI, R [1985], "A Phenomenological Theory of Transformation Superplasticity", *Ing. Arch.* , **51** : 287-299 .

TANAKA, K. [1986], "A Thermomechanical Sketch of Shape Memory Effect: One Dimensional Tensile Behavior", *Res. Mech.*, **18**: 251-263.

VANDERMEER, R.A., OGLE, J.C., AND NORTHCUTT, W.G. JR. [1981], "A Phenomenological Study of the Shape Memory Effect in Polycrystalline Uranium-Niobium Alloys," *Metallurgical Trans. A*, **12A**: 733-741.

ZIENKIEWICZ, O.C. & TAYLOR, R.L. [1989], "The Finite Element Method, Vol 1.", 4th ed., McGraw-Hill, London.